Confirmation of Slow Waves in a Crosstie Overlay Coplanar Waveguide and Its Applications to Band-Reject Gratings and Reflectors

TE-HUI WANG, STUDENT MEMBER, IEEE, AND TATSUO ITOH, FELLOW, IEEE

Abstract—**The slow-wave propagation along a new crosstie overlay slow-wave coplanar waveguide has been investigated both theoretically and experimentally. A slow-wave factor observed agrees reasonably well with the theoretical prediction. This structure is used for construction of frequency-selective distributed Bragg reflectors (DBR's) of compact size. The effect of conductor loss is considered. A doubly periodic band-reject grating has been created from the DBR's and the band-reject phenomenon was observed as predicted. To improve passband characteristics of the grating, a monolithic slow-wave Chebyshev reflector was designed and fabricated. Agreement between theory and preliminary experiment has been confirmed. Based on this theory, a new slow-wave reflector with improved characteristics is proposed and examined. A respectable slow-wave factor and a drastic reduction of conductor loss have been predicted.**

I. INTRODUCTION

ONE OF THE MOST important requirements in the design of monolithic microwave integrated circuits (MMIC's) is minimizing the monolithic circuit size. Conventional printed line circuits cannot reduce the guide wavelength λ_g by more than $\sqrt{\epsilon_r}$ (ϵ_r being the relative dielectric constant of the transmission medium) from the free-space wavelength λ_0. A slow-wave transmission line provides a possible remedy. Conventional MIS and Schottky slow-wave structures are inherently lossy [1], although the latter can provide the possibility of electronically tuning the slow-wave factor by the dc bias applied to the wave-propagating electrode. Recently, Hasegawa proposed a new crosstie coplanar waveguide (CTCPW) slow-wave structure in which the wave attenuation is due predominantly to the conductor loss [1]. More recently, Wang and Itoh [2] have suggested a modification of Hasegawa's CTCPW and proposed a different crosstie overlay slow-wave structure, which is believed more adaptable for monolithic circuit integration. Instead of buried crossties, overlay crossties were used. As shown in Fig. 1, both CPW (coplanar waveguide) and microstrip line versions of the new slow-wave structure can be realized by the overlay technique.

The objective of the present work is to create a physically short grating by means of this slow-wave structure. Grating structures are found useful in millimeter-wave integrated circuit applications such as band-reject filters [3], [4] and distributed Bragg reflector (DBR) oscillators [5]. In such applications, the gratings would be operated in stopbands, corresponding to Bragg reflection, in order to produce strong reflections. Because the band-reject filters or DBR structures made of the conventional dielectric waveguide and printed line tend to be electrically and physically long, they are not very suitable for monolithic integrated circuits. However, if such periodic structures can be made of the proposed crosstie slow-wave structures, the physical size of the grating can be made smaller while the electrical length will still be long enough to observe grating effects. In this study, the dispersive characteristics of the new crosstie slow-wave CPW's were confirmed experimentally. Then a distributed Bragg reflector was made of the new overlay crosstie mechanism to realize a slow-wave band-reject grating (see Fig. 2) with a physically short dimension. From the transmission and reflection characteristic measurements, a band-reject phenomenon was confirmed. Although such frequency-selective band-reject gratings can give a strong stopband, their passbands may have ripples which are excessive for many applications. In order to obtain better control of the passband ripple at a reasonably low level, we created a slow-wave reflector from the new crosstie overlay CPW's which has a prescribed stopband as well as prescribed Chebyshev passbands. The design procedure is based on the formulation proposed by Cohn [6] for an approximate synthesis of distributed stepped-impedance transformers. A monolithic slow-wave Chebyshev reflector has been designed and fabricated. Although the transmission and reflection characteristic measurements indicate that a band-reject phenomenon was confirmed, a somewhat high ohmic loss due to the large skin current densities on the surface of the crosstie strips and the center conductor of the CPW caused a degradation of the reflector's performance.

Manuscript received March 29, 1988; revised July 8, 1988. This work was supported by the U.S. Army Research Office under Contract DAAG-84-K-0076.

T.-H. Wang was with the Department of Electrical and Computer Engineering, University of Texas at Austin, Austin, TX. He is now with the Chung Shun Institute of Science and Technology, Lung Tan, Taiwan.

T. Itoh is with the Department of Electrical and Computer Engineering, University of Texas at Austin, Austin, TX 78712.

IEEE Log Number 8823772.

0018-9480/88/1200-1811$01.00 ©1988 IEEE

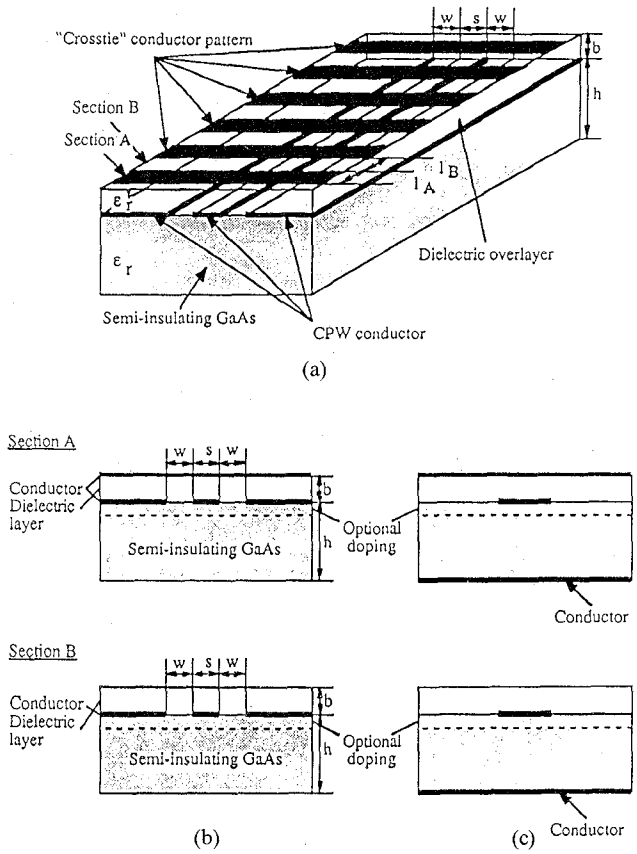

Fig. 1. Crosstie overlay CPW and microstrip slow-wave structures. (a) CPW. (b) Cross section of CPW. (c) Cross section of microstrip.

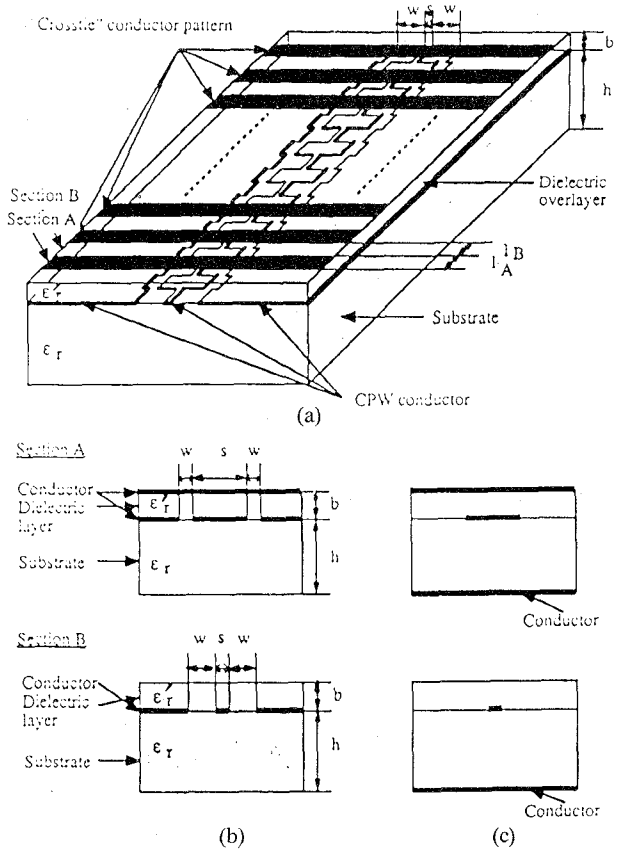

Fig. 3. Modified crosstie overlay CPW and microstrip slow-wave structures. (a) CPW. (b) Cross section of CPW. (c) Cross section of microstrip.

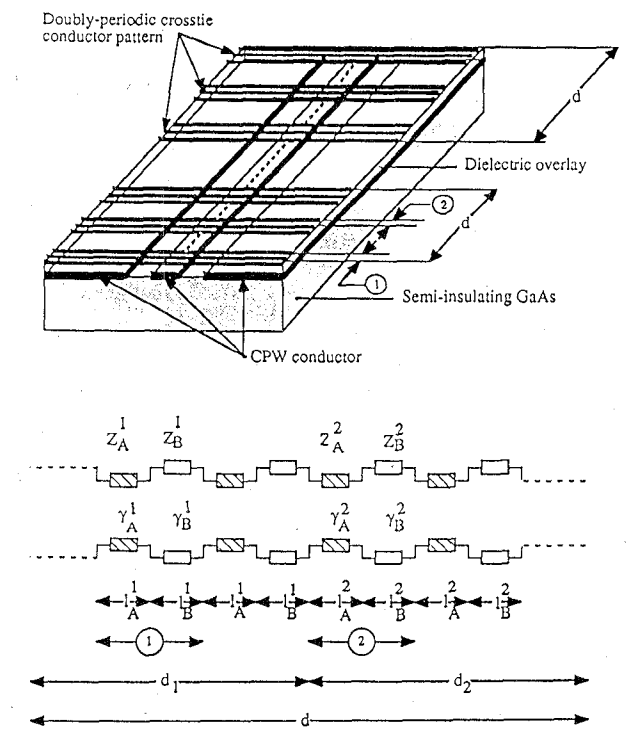

Fig. 2. Schematic and equivalent circuit of doubly periodic band-reject grating.

In order to reduce ohmic loss to an acceptable level, a modification of the slow-wave CPW presented in [2] has been made based on a mechanism similar to that described in [7] and is proposed as the new building block of the slow-wave reflector circuits. Fig. 3 is the schematic of the modified crosstie overlay slow-wave CPW. As shown in this figure, the same modification can also be applied to the microstrip version. Instead of using a thin dielectric overlay to generate a cascaded chain of large capacitive and inductive sections, a much thicker dielectric overlay and modulated cross-sectional confirmations of CPW in the constituent sections A and B are adopted in this work. Since the slow-wave factor in the periodic crosstie overlay CPW mainly depends on $\sqrt{Z_B/Z_A}$ (Z_A and Z_B being the characteristic impedances of the constituent sections A and B, respectively), the large value of the slow-wave factor will be maintained in spite of a much thicker dielectric overlay if different cross-sectional configurations of the CPW in sections A and B are appropriately chosen. The spatial separation of electric and magnetic energies is not changed while the skin current densities flowing on the crosstie strips and center conductor of the CPW are reduced. It is conceivable that the slow-wave reflector proposed in this paper will be able to provide a reasonably short physical length as well as a lower level of attenuation inside the passbands. This is useful for implementation of a possible high-Q circuit in the passive monolithic microwave and millimeter-wave integrated circuits.

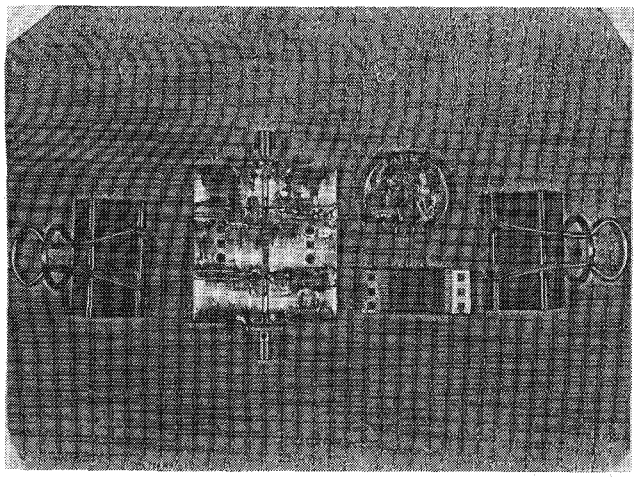

Fig. 4. Photograph of the disassembled crosstie overlay slow-wave CPW.

II. Dispersive Characteristics of New Crosstie Overlay Slow-Wave CPW

The theoretical treatment of the new crosstie overlay slow-wave CPW (Fig. 1) has been described in [2]. In the present experiment, a CPW pattern was photoetched on a prethinned 15 μm Cu-clad Epsilam-10 substrate surface with $\epsilon_r = 10.2$ and $h = 0.635$ mm (h being the thickness of substrate). The center conductor width of the CPW is $s = 0.15$ mm and the slot width is $w = 0.745$ mm. Twenty periods of metal crossties were photoetched on another prethinned 15 μm Cu-clad microwave substrate surface with $\epsilon_r = 2.5$ and $h = 0.762$ mm. The lengths of the constituent sections in each period are $l_A = 0.30$ mm (with crosstie strip) and $l_B = 0.30$ mm (without crosstie strip). By using the spun-on technique, a 3.0 μm thick DuPont PI-2556 polyimide ($\epsilon_r' = 3.5$) layer was coated on the surface of periodic crossties as the dielectric overlay. After the polyimide was properly cured, construction of a crosstie slow-wave CPW was accomplished by attaching the substrate with the CPW and another with the crossties face-to-face. Mechanical pressure was applied to make sure that the two pieces had good contact.

The experimental verification of the slow-wave factor in the crosstie overlay slow-wave CPW was performed by measuring the phase shift using a Hewlett-Packard network analyzer. Fig. 4 is a photograph of a disassembled crosstie overlay slow-wave CPW. Sections of 50 Ω conventional CPW were connected at the input and output ends. In measurement, these 50 Ω CPW's were connected directly to form a calibration reference. The measured values of the slow-wave factor are plotted against frequency in Fig. 5. The measured slow-wave factor of a simple CPW without a crosstie pattern is also shown for comparison. These results indicate slow-wave propagation with a negligible dispersion. Measured values of the slow-wave factor are close to the theoretical values shown by the solid line. The cause of the discrepancy includes the existence of an air gap due to the thickness of the crossties. The measured values of the attenuation constant are plotted against frequency in Fig. 6. The measured attenuation constant of

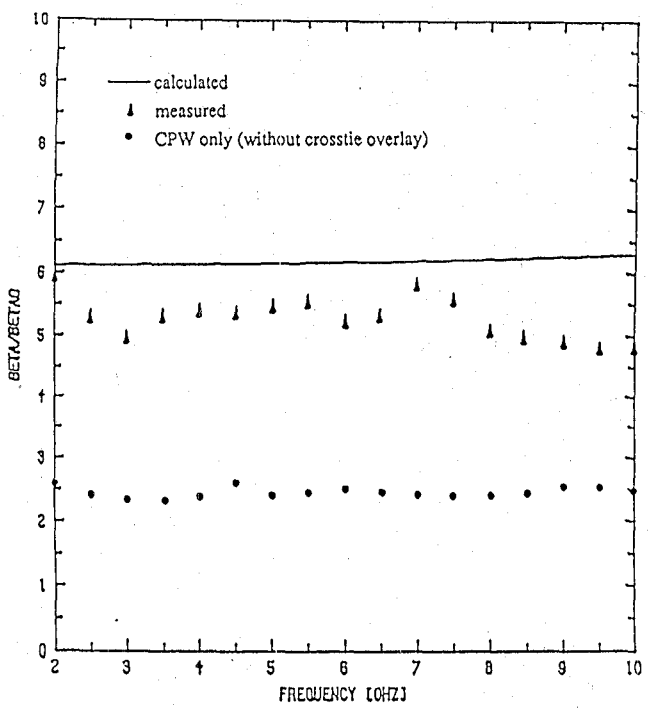

Fig. 5. SLow-wave factor (β/β_0) of the crosstie overlay slow-wave CPW.

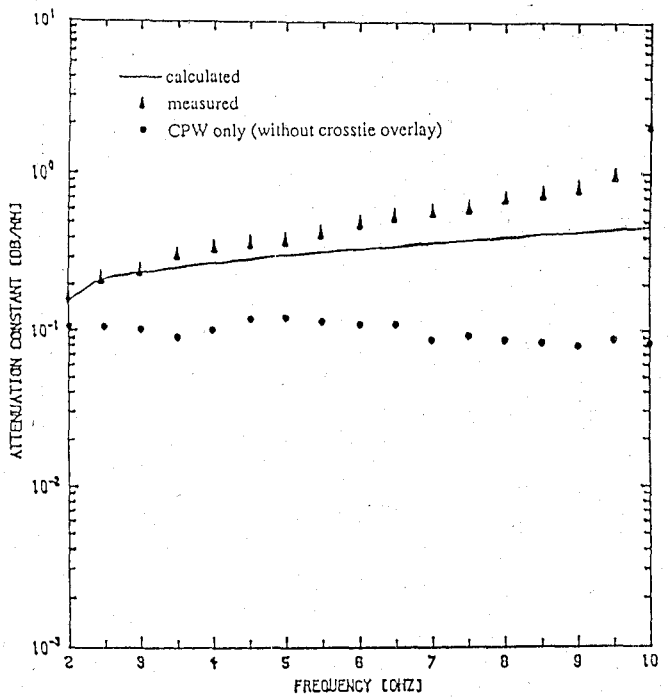

Fig. 6. Attenuation constant of the crosstie overlay slow-wave CPW.

a simple CPW without a crosstie pattern is also shown for comparison. As shown in this figure, the crosstie overlay slow-wave CPW exhibits higher attenuation per unit physical length than the simple CPW due to the existence of the crosstie conductors. However, the difference is much smaller if the values are compared with respect to the guide wavelength. Measured values of the attenuation constant agree reasonably with the theoretical values shown by the solid line.

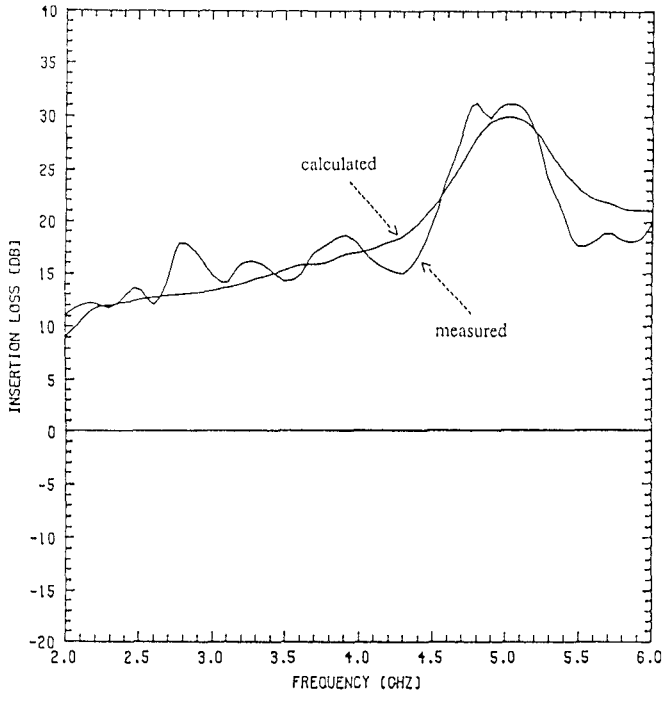

Fig. 7. Insertion loss of the crosstie overlay band-reject grating.

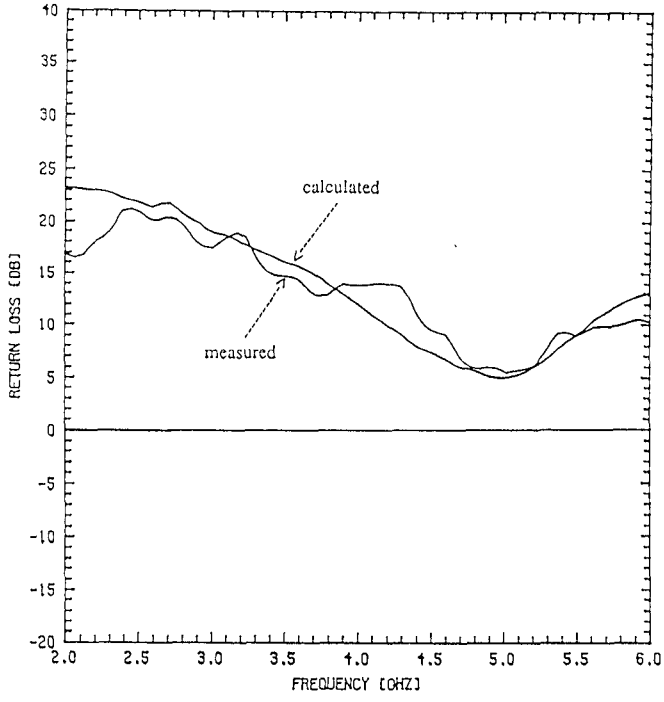

Fig. 8. Return loss of the crosstie overlay band-reject grating.

III. Frequency-Dependent Reflection and Transmission Characteristics of the Band-Reject Grating

As shown in Fig. 2, we have created a band-reject grating with its period comparable to the guide wavelength from the "uniform" crosstie overlay slow-wave CPW's. This "uniform" line itself is a periodic structure with its period much shorter than the wavelength and is designed as described in the previous section. Hence, the band-reject grating is physically a doubly periodic structure [8]. As shown in this figure, one period of the grating consists of two sections of crosstie overlay slow-wave CPW's with different slow-wave factors and characteristic impedances. The slow-wave CPW in the section d_1 consists of sections A and B (defined in Fig. 1) 0.10 mm and 0.12 mm long, respectively, while the one in section d_2 is made of 0.12 mm and 0.10 mm long sections. Hence, with reference to Fig. 2, $l_{A^1} = 0.10$ mm and $l_{B^1} = 0.12$ mm while $l_{A^2} = 0.12$ mm and $l_{B^2} = 0.10$ mm. Section d_1 contains 17 periods of $l_{A^1} + l_{B^1}$ whereas d_2 contains 17 periods of $l_{A^2} + l_{B^2}$. Hence, the length of the period d of the band-reject grating is 7.48 mm. Section d_1 has a higher characteristic impedance than section d_2. It should be noted that before designing the grating, the slow-wave factor is recalculated to include the air gap effect so that the discrepancy between the calculated and the measured slow-wave factor is much smaller than the one observed in Fig. 5.

Following fabrication procedures similar to those for the crosstie overlay slow-wave CPW, a 9.5 period long grating with a total length of 7.106 cm ($9.5 \times d$) was finally obtained. A section of 50 Ω conventional CPW was used at the input and output ends, respectively, as the test fixture. The same setup as that in the slow-wave factor measurement was exploited for the characterization of grating reflection and transmission properties. Fig. 7 shows the calculated and the measured values of insertion loss, and Fig. 8 shows the return loss plotted against frequency of the fabricated grating. From these two figures, a band-rejection phenomenon can be clearly recognized. The center frequency of the stopband is 4.95 GHz in experiment and 5.03 GHz in theory. The difference is about 1.6 percent. The 3 dB bandwidth of the stopband is 0.56 GHz in experiment and 0.50 GHz in theory. The difference is caused not only by errors in fabrication but also by the fact that the junction susceptance between two transmission lines was not taken into account in the theoretical calculation. The Q value inside the stopband is around 8.8 in experiment and 10 in theory. The peak insertion loss and the return loss in the stopband are 31 dB and 6 dB in experiment and 30 dB and 5 dB in theory, respectively. The slow-wave factor of this band-reject grating is about 4. From the above-mentioned quantities, our theoretical and experimental results are in good agreement. However, the somewhat higher insertion loss in the passband due to the attenuation of whole crosstie slow-wave CPW sections and the discontinuity effects, including radiation loss in the test device, requires further reduction for practical applications. In the following section, a slow-wave Chebyshev reflector is proposed and synthesized for this purpose.

IV. Synthesis of Slow-Wave Chebyshev Reflector Prototypes

The transmission-line prototype circuit used in the design of a slow-wave Chebyshev reflector is the equal-electrical-length quarter-wave step-impedance filter shown in Fig. 9. It is a distributed filter consisting of n cascaded line

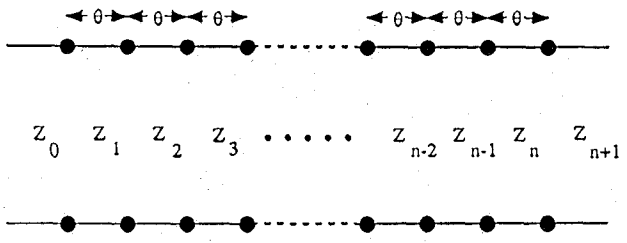

Fig. 9. Equal-electrical-length transmission-line equivalent circuit for slow-wave Chebyshev reflector prototype.

elements; each element corresponds to a resonator in the conventional filter design. The elements, consisting of an appropriate length of slow-wave structure as shown in Fig. 1 with characteristic impedances Z_r ($r=1,2,3,\cdots,n$), are assumed to have a length of $L_r=(\lambda_{g^0})_r/4$, where $(\lambda_{g^0})_r$ is the guide wavelength of the rth impedance step at the stopband center frequency. The electric response of this transmission-line structure depends on the impedances of the unit elements. For electromagnetic waves propagating along the line, the impedance differences between the unit elements yield reflected waves which, after appropriate arrangement, will accumulate to cause the band-reject phenomenon to take place at the desired frequencies. Based on Cohn's [6] approximate synthesis procedure for stepped-impedance transformers by considering only the first-order reflection effects, a scheme similar to the one presented in [9] was employed to synthesize a slow-wave Chebyshev reflector with the prescribed characteristics. After the synthesis of a prototype of the type shown in Fig. 9, the value of the characteristic impedance for each impedance step was scaled up to facilitate the realization from the crosstie overlay slow-wave CPW's.

For a chosen crosstie overlay slow-wave CPW configuration, the propagation constants and the characteristic impedances of each constituent section A (with crosstie strip) and B (without crosstie strip) at the stopband center frequency were calculated by utilizing the standard spectral-domain method [10]. The attenuation constants due to dielectric loss in both sections A and B were assumed negligibly small, while the attenuation constants due to ohmic loss were calculated from Wheeler's incremental inductance formula [11]. In the meantime, we assumed that the propagation constants in both sections A and B were not affected by the attenuation due to conductor loss. The information for sections A and B was then used in [2, eq. (2)]. The lengths l_A and l_B of the constituent sections A and B for each impedance step were thus determined. It is important that the operating wavelength be sufficiently longer than the period l ($=l_A+l_B$) of the period crosstie overlay CPW so that the structure will simulate an uniform transmission line. Finally, [2, eq. (1)] was used to obtain the guide wavelength at the stopband center frequency $(\lambda_{g^0})_r$ for each impedance step r, and therefore the length L_r for each impedance step that brings the entire structure into synchronism. It is noted that due to the almost nondispersive feature of the crosstie overlay CPW's, the synthesis of the slow-wave Chebyshev reflector prototype depicted above does not include the effects of the stopband-width shrinkage that will occur due to dispersion.

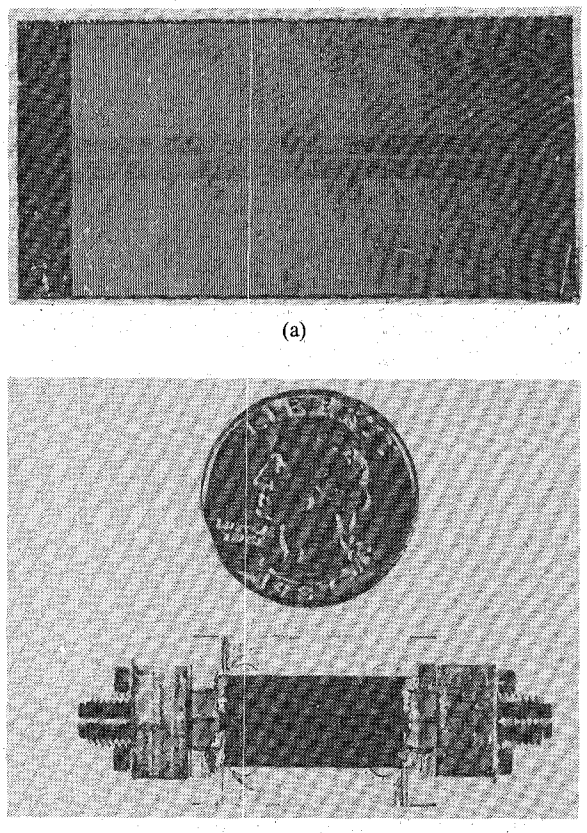

(a)

(b)

Fig. 10. Photograph of the slow-wave Chebyshev reflector. (a) Device chip. (b) Device and test jig.

V. Preliminary Experimental Results of the Slow-Wave Chebyshev Reflector

Referring to Fig. 1 for experimental simplicity, a monolithic crosstie overlay slow-wave CPW with $s=0.15$ mm, $w=0.745$ mm, $b=0.001$ mm, $h=0.35$ mm, $\epsilon_r=12.9$ (semi-insulating GaAs), $\epsilon_r'=6.5$ (Si_3N_4) and Au (conductors of CPW and crosstie strips) $=0.0015$ mm has been adopted to serve as the building block of our preliminary slow-wave Chebyshev reflector circuit. Thirteen impedance steps were cascaded to synthesize the Chebyshev reflector with the prescribed characteristics listed as follows: (1) stopband frequency = 9 GHz, (2) maximum stopband attenuation = 20 dB, (3) equiripple level in passbands = 0.5 dB, and (4) equiripple fractional bandwidth = 0.4. For convenience of measurement, two three-section quarter-wave impedance transformers were connected to both the input and output ends of the reflector so that the problem of impedance matching with external 50 Ω measuring systems was eliminated. Table I shows details of the values Z, l_A, l_B, and L for each impedance step of the entire circuit. Fig. 10 is a photograph of the device embedded in a 50 Ω test jig. Figs. 11 and 12 show the calculated and measured insertion loss and return loss, respectively, of the

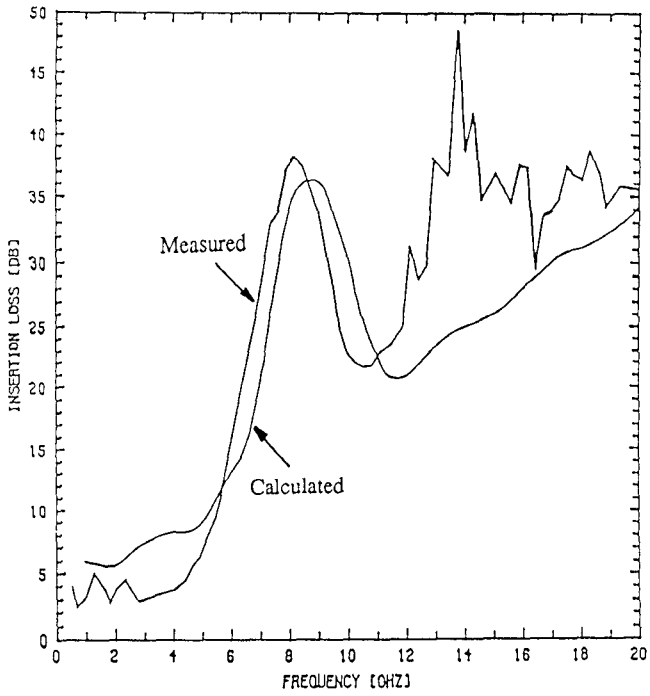

Fig. 11. Insertion loss of the preliminary slow-wave Chebyshev reflector.

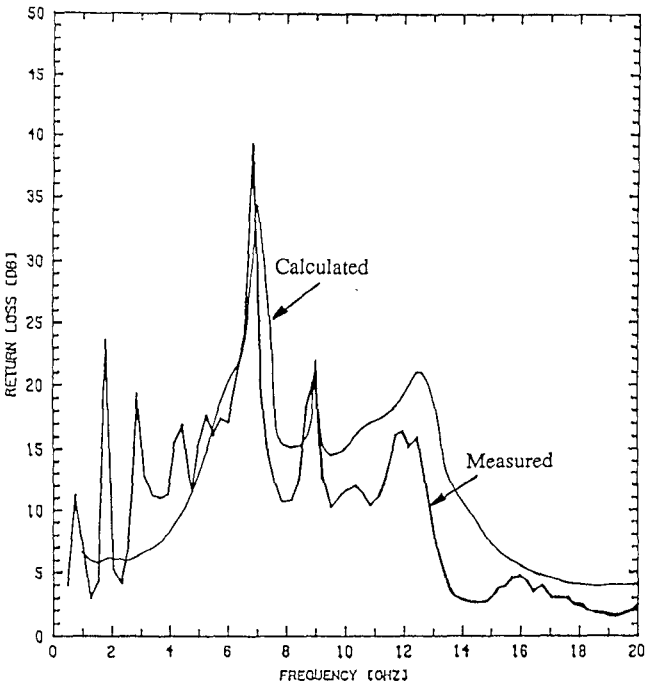

Fig. 12. Return loss of the preliminary slow-wave Chebyshev reflector.

slow-wave Chebyshev reflector. In the calculated curves, the effect of the ohmic loss of the gold conductor (resistivity $= 2.35 \times 10^{-6}$ $\Omega \cdot$cm) has been included. From these two figures, the center frequency of the stopband is 8.15 GHz in experiment and 8.85 GHz in theory. The difference is about 8 percent. The difference is caused not only by the errors in fabrication but also by the fact that the high-order reflections in each impedance step were not taken into account in the calculation of each junction's

TABLE I
DETAILED INFORMATION ON Z, l_A, l_B, AND L OF THE SLOW-WAVE CHEBYSHEV REFLECTOR AND QUARTER-WAVE IMPEDANCE TRANSFORMERS

# of impedance steps \ impedances & lengths	Z (Ω)	l A (mm)	l B (mm)	L (mm)
1 (imped transf.)	37.31	.0039	.0961	1.4
2 (")	24.50	.0093	.0907	1.0
3 (")	16.08	.0199	.0801	0.7
4 (input section)	12.00	.0312	.0688	0.6
5 (Cheby. reflec.)	21.67	.0118	.0882	0.9
6 (")	16.21	.0197	.0803	0.7
7 (")	22.89	.0106	.0894	0.9
8 (")	15.43	.0213	.0787	0.7
9 (")	23.82	.0099	.0901	1.0
10 (")	15.01	.0223	.0777	0.7
11 (")	24.17	.0096	.0904	1.0
12 (")	15.01	.0223	.0777	0.7
13 (")	23.82	.0099	.0901	1.0
14 (")	15.43	.0213	.0787	0.7
15 (")	22.89	.0106	.0894	0.9
16 (")	16.21	.0197	.0803	0.7
17 (")	21.67	.0118	.0882	0.9
18 (output section)	12.00	.0312	.0688	0.6
19 (imped. transf.)	16.08	.0199	.0801	0.7
20 (")	24.50	.0093	.0907	1.0
21 (")	37.31	.0039	.0961	1.4

VSWR. The peak insertion loss in the stopband is 38 dB in experiment and 35.5 dB in theory. The minimum return loss in the stopband is 11 dB in experiment and 15 dB in theory. The poor return loss inside the passband comes from the narrow-bandwidth impedance transformers. The slow-wave factor of this reflector at the stopband center frequency is about 10.5. The physical and electrical lengths of the slow-wave reflector are 10.8 mm and 19.99 rad, respectively. From the above discussion, our theoretical and experimental results agree reasonably well. However, the detrimental ohmic loss diminishes the usefulness of the reflector. In order to reduce the ohmic loss of the circuit such that a higher Q value can be obtained, a modified crosstie overlay slow-wave CPW, shown in Fig. 3, is proposed and examined in the following section.

VI. PREDICTED CHARACTERISTICS OF THE MODIFIED SLOW-WAVE CHEBYSHEV REFLECTOR

As Fig. 3 shows, a modified crosstie overlay slow-wave CPW with $s_A = 3.0$ mm, $w_A = 0.2$ mm, $s_B = 0.1$ mm, $w_B = 1.6$ mm, $b = 0.02$ mm, $h = 0.254$ mm, $\epsilon_r = 9.7$ (alumina), $\epsilon_r' = 3.5$ (polyimide), and Au = 0.004 mm is selected as the new building block of our slow-wave Chebyshev reflector circuit. The prescribed characteristics are as follows: (1) stopband center frequency = 5 GHz, (2) maximum stopband attenuation = 10 dB, (3) equiripple level in passbands = 0.5 dB, and (4) equiripple fractional bandwidth = 0.25. After the synthesis of the circuit, the number of required impedance steps is 15. Table II presents details of the values Z, l_A, l_B, and L for each impedance step. Figs. 13 and 14 show the predicted insertion loss and return loss, respectively, of the new slow-wave Chebyshev reflector. As

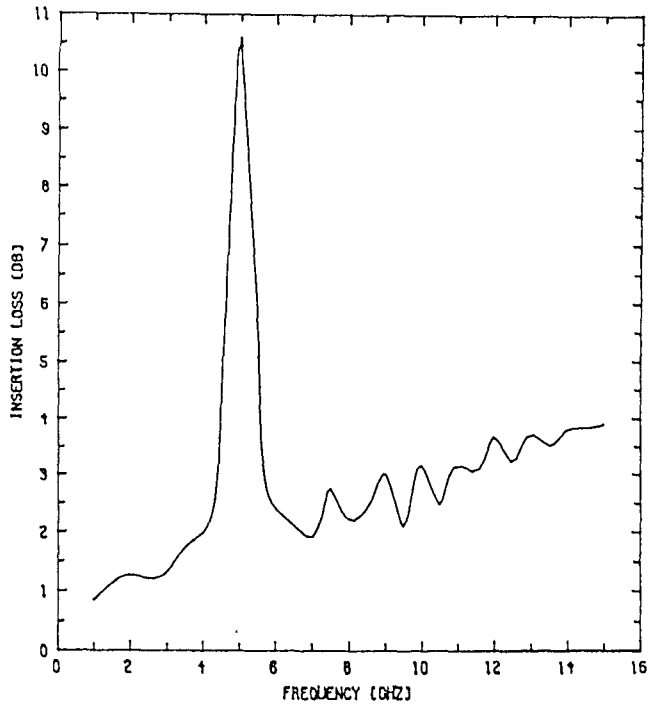

Fig. 13. Predicted insertion loss of the modified slow-wave Chebyshev reflector.

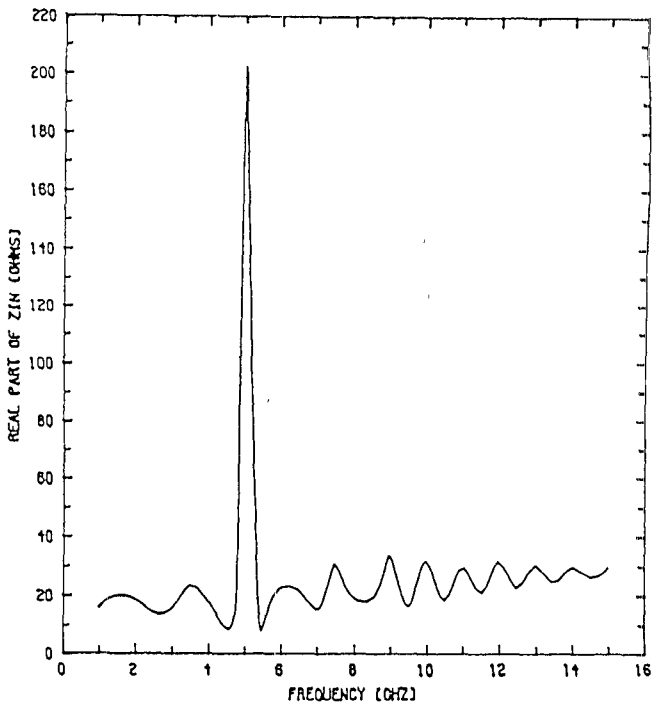

Fig. 15. Real part of the input impedance of the modified slow-wave Chebyshev reflector.

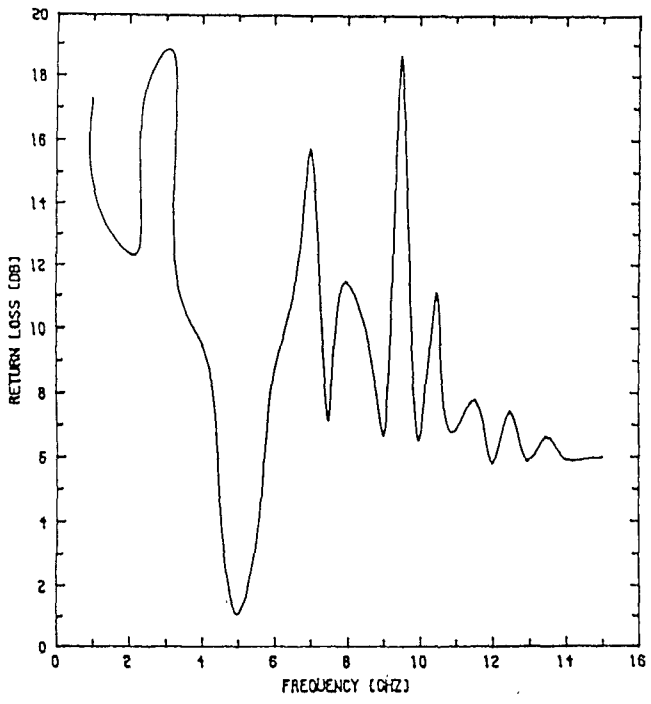

Fig. 14. Predicted return loss of the modified slow-wave Chebyshev reflector.

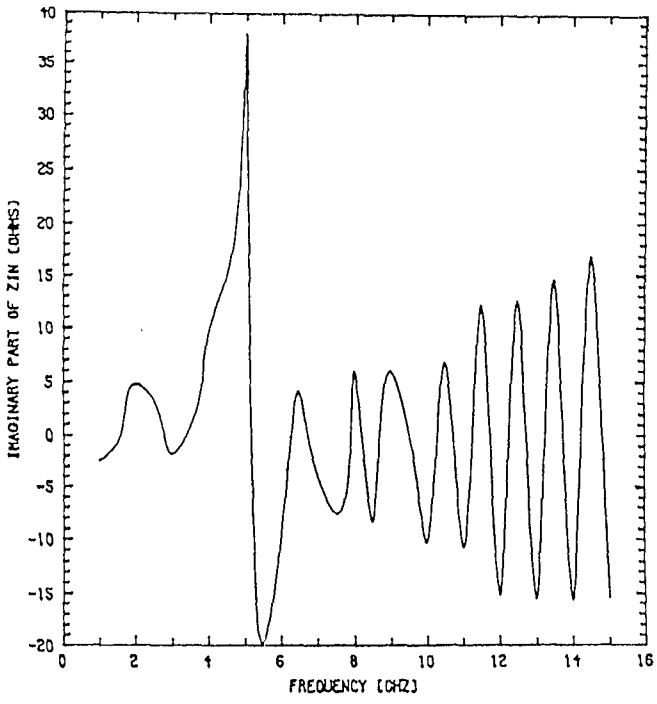

Fig. 16. Imaginary part of the input impedance of the modified slow-wave Chebyshev reflector.

Fig. 13 shows, a somewhat higher ripple size (about 3–4 dB) in the upper passband due to conductor loss could be further reduced by appropriate adjustment of the CPW cross-sectional configuration and dielectric overlay thickness. Figs. 15 and 16 show the real and imaginary parts of the input impedance, respectively, of the new slow-wave reflector. The load impedance connected to the output end of the reflector is 13 Ω. The slow-wave factor of this reflector is about 9. The physical and electrical lengths of the new slow-wave reflector are 24.1 mm and 23.46 rad, respectively. Fabrication of this new slow-wave reflector circuit is under way.

TABLE II
DETAILED INFORMATION ON Z, l_A, l_B, AND L OF THE MODIFIED SLOW-WAVE CHEBYSHEV REFLECTOR

# of impedance steps \ impedances & lengths	Z (Ω)	l_A (mm)	l_B (mm)	L (mm)
1	21.90	.0227	.0773	1.7
2	18.91	.0284	.0716	1.5
3	22.27	.0221	.0779	1.7
4	18.63	.0291	.0709	1.5
5	22.55	.0216	.0784	1.7
6	18.45	.0295	.0705	1.5
7	22.70	.0214	.0786	1.7
8	18.39	.0296	.0704	1.5
9	22.70	.0214	.0786	1.7
10	18.45	.0295	.0705	1.5
11	22.55	.0216	.0784	1.7
12	18.63	.0291	.0709	1.5
13	22.27	.0221	.0779	1.7
14	18.91	.0284	.0716	1.5
15	21.90	.0227	.0773	1.7

VII. CONCLUSIONS

The slow-wave propagation along a new crosstie overlay slow-wave structure has been experimentally confirmed. Based on this new slow-wave structure, the distributed Bragg reflection mechanism was introduced to realize a band-reject grating. From measurements of the reflection and transmission characteristics, a band-reject phenomenon was observed as predicted. In order to improve the passband characteristics of the band-reject grating, a monolithic slow-wave Chebyshev reflector was designed and fabricated. Agreement between theory and preliminary experiment has been confirmed. Based on this theory, a new slow-wave Chebyshev reflector with improved characteristics is proposed and fabricated. The simplicity of the design procedure, lower loss, and better control in the passband ripple size make the structure a viable candidate for the distributed Bragg reflector (DBR) oscillator application.

ACKNOWLEDGMENT

The authors would like to thank Dr. H. Q. Tserng and Dr. N. Camilleri of Texas Instruments, Dallas, TX, for their help in fabricating the monolithic reflector circuit and performing device characterization.

REFERENCES

[1] S. Seki and H. Hasegawa, "Cross-tie slow-wave coplanar waveguide on semi-insulating GaAs substrate," *Electron. Lett.*, vol. 17, no. 25, pp. 940–941, Dec. 1981.
[2] T. H. Wang and T. Itoh, "Compact grating structure for application to filters and resonators in monolithic microwave integrated circuits," *IEEE Trans. Microwave Theory Tech.*, vol. MTT-35, pp. 1176–1181, Dec. 1988.
[3] T. Itoh, "Application of gratings in a dielectric waveguide for leaky-wave antennas and band-reject filters," *IEEE Trans. Microwave Theory Tech.*, vol. MTT-25, pp. 1134–1138, Dec. 1977.
[4] M. Tsutsumi, T. Ohira, T. Yamaguchi, and N. Kumagai, "Reflection of millimeter waves by a corrugated dielectric slab waveguide," *Proc. IEEE*, vol. 68, pp. 733–734, June 1980.
[5] T. Itoh and F. Hsu, "Distributed Bragg reflector Gunn oscillators for dielectric millimeter-wave integrated circuits," *IEEE Trans. Microwave Theory Tech.*, vol. MTT-27, pp. 514–518, May 1979.
[6] S. B. Cohn, "Optimum design of stepped transmission-line transformers," *IRE Trans. Microwave Theory Tech.*, vol. MTT-3, pp. 16–21, Apr. 1955.
[7] E. M. Bastida and G. P. Donzelli, "Periodic slow-wave low-loss structures for monolithic GaAs microwave circuits," *Electron. Lett.*, vol. 15, no. 19, pp. 581–582, 1979.
[8] S. T. Peng, J. M. Dong, and L. M. Wang, "Wave interaction in doubly periodic structures," in *1985 IEEE MTT-S Int. Microwave Symp. Dig.*, pp. 131–134.
[9] D. C. Park, G. L. Matthaei, and M. S. Wei, "Bandstop filter design using a dielectric waveguide grating," *IEEE Trans. Microwave Theory Tech.*, vol. MTT-33, pp. 693–702, Aug. 1985.
[10] T. Itoh, "Spectral domain immittance approach for dispersion characteristics of generalized printed transmission lines," *IEEE Trans. Microwave Theory Tech.*, vol. MTT-28, pp. 733–736, July 1980.
[11] H. A. Wheeler, "Formulas for the skin effect," *Proc. IRE*, vol. 30, pp. 412–424, 1942.

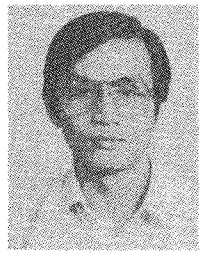

Te-Hui Wang (S'86) was born in Taichung, Taiwan, Republic of China, on May 16, 1954. He received the B.Sc. degree in physics from National Tsing Hua University, Taiwan, in 1977, the M.E. degree from the Tatung Institute of Technology, Taiwan, in 1981, and the Ph.D. degree from the University of Texas at Austin, in 1988.

He is now with the Chung Shun Institute of Science and Technology, Lung Tan, Taiwan. His current research interests include the analysis and design of microwave and millimeter-wave components.

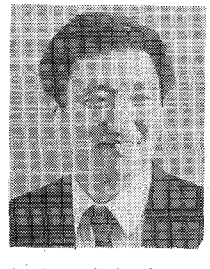

Tatsuo Itoh (S'69–M'69–SM'74–F'82) received the Ph.D. degree in electrical engineering from the University of Illinois, Urbana, in 1969.

From September 1966 to April 1976, he was with the Electrical Engineering Department, University of Illinois. From April 1976 to August 1977, he was a Senior Research Engineer in the Radio Physics Laboratory, SRI International, Menlo Park, CA. From August 1977 to June 1978, he was an Associate Professor at the University of Kentucky, Lexington. In July 1978, he joined the faculty at the University of Texas at Austin, where he is now a Professor of Electrical Engineering and Director of the Electrical Engineering Research Laboratory. During the summer of 1979, he was a guest researcher at AEG-Telefunken, Ulm, West Germany. Since September 1983, he has held the Hayden Head Centennial Professorship of Engineering at the University of Texas. In September 1984, he was appointed Associated Chairman for Research and Planning of the Electrical and Computer Engineering Department. He also holds an Honorary Visiting Professorship at the Nanjing Institute of Technology, China.

Dr. Itoh is a member of the Institute of Electronics and Communication Engineers of Japan and Sigma Xi. He is a member of Commission B and Chairman of Commission D of USNC/URSI. He served as the Editor of IEEE TRANSACTIONS ON MICROWAVE THEORY AND TECHNIQUES for 1983–1985. He serves on the Administrative Committee of IEEE Microwave Theory and Techniques Society. Dr. Itoh is a Professional Engineer registered in the state of Texas.